ORIGINAL ARTICLE

Metabolomic evaluation of Mitomycin C and rapamycin in a personalized treatment of pancreatic cancer

Alicia Navarrete[1], Emily G. Armitage[1], Monica Musteanu[2], Antonia García[1], Annalaura Mastrangelo[1], Renata Bujak[1,3], Pedro P. López-Casas[2], Manuel Hidalgo[2,] & Coral Barbas[1]

[1]CEMBIO (Center for Metabolomics and Bioanalysis), Facultad de Farmacia, Universidad CEU San Pablo, Campus Montepríncipe, Boadilla del Monte, 28668, Madrid, Spain
[2]CNIO (Spanish National Cancer Research Centre), E-28029, Madrid, Madrid, Spain
[3]Department of Biopharmacy and Pharmacodynamics, Medical University of Gdansk, Al. Hallera 107, Gdansk, 80-416, Poland

Abstract

In a personalized treatment designed for a patient with pancreatic cancer resistant to other treatments, the success of Mitomycin C (MMC) has been highlighted. This was revealed in a murine xenograft tumor model encompassing pancreatic adenocarcinoma cells extracted from the patient. The patient was found to exhibit a biallelic inactivation of the *PALB2* gene, involved in DNA repair in addition to another mutation in the *TSC2* gene that induces susceptibility of the tumor to therapeutic targets of the PI3K-mTOR pathway. The aim of the study was to apply metabolomics to elucidate the modes of action of each therapy, suggesting why MMC was so successful in this patient and why it could be a more popular choice in future pancreatic cancer treatment. The effectiveness of MMC compared to rapamycin (RM), another relevant therapeutic agent has been evaluated through liquid- and gas-chromatography mass spectrometry-based metabolomic analyses of the xenograft tumors. The relative concentrations of many metabolites in the xenograft tumors were found to be increased by MMC relative to other treatments (RM and a combination of both), including a number that are involved in central carbon metabolism (CCM). Metabolic fingerprinting revealed statistically significantly altered pathways including, but not restricted to, the pentose phosphate pathway, glycolysis, TCA cycle, purine metabolism, fatty acid biosynthesis, in addition to many significant lipid and amino acid alterations. Given the genetic background of the patient, it was expected that the combined therapy would be most effective; however, the most effective was MMC alone. It is proposed that the effectiveness of MMC is owed to its direct effect on CCM, a vital region of tumor metabolism.

Abbreviations

AAALAC, Association for Assessment and Accreditation of Laboratory Animal Care; CCM, central carbon metabolism; CV1, cross-validation; FAME, fatty acid methyl ester; FAS, Fatty acid synthase; GC-MS, gas chromatography–mass spectrometry; IACUC, Institutional Animal Care and Use Committee; LC-MS, liquid chromatography mass spectrometry; MMC, Mitomycin C; NT, not treated; OG, other groups; OPLS-DA, orthogonal partial least squares regression discriminant analysis; PCA, principal components analysis; QC, quality controls; RM, rapamycin; TCA, tricarboxylic acid; TGI, tumor growth inhibition.

Introduction

Despite significant advances in understanding the molecular basis of pancreatic cancer, there has been little progress in the treatment of the disease (Jones et al. 2008; Hidalgo 2010). Since pancreatic cancer is symptomless in its early stages, diagnosis often occurs after metastasis to other organs. Therefore, treatment of pancreatic cancer usually begins with surgery to remove the main risk and patients are subsequently treated with either radio- or chemotherapy. Treatments currently employed are not always definitive and may not be achievable, depending on the aggressiveness of the tumor.

Approximately 10% of all cases of pancreatic cancer occur due to a genetic predisposition to the disease (Vincent et al. 2011). For example, as part of our studies in personalized treatment of patients with pancreatic cancer, we identified a patient who exhibited resistance to the commonly used treatment for pancreatic cancer: gemcitabine, and had only a 3-month life expectancy. The patient was treated with Mitomycin C (MMC) selected due to its success on a murine xenograft model (Avatar model) generated from pancreatic adenocarcinoma cells extracted from the patient. Following treatment, the tumor marker CA19-9 was restored to normality in 3 years and the patient was apparently symptom free. To reveal the mode of action of MMC in this case, genomic studies were undertaken, revealing that the patient exhibited a biallelic inactivation of the *PALB2* gene, which is involved in DNA repair. This was further proved by testing the treatment with the wild-type *PALB2* gene, which showed resistance to MMC. We showed that this mutation is associated with susceptibility to alkylating agents such as MMC, and in fact that patient had a very good clinical response and survival with this class of agents. In addition to this mutation, there was another mutation in the *TSC2* gene (Villarroel et al. 2011). It has been previously shown that mutations in this gene result in hyperactivation of the phosphoinositide 3-kinase/ mammalian target of rapamycin (PI3K-mTOR) pathway and confer susceptibility to inhibitors of these targets (Franz and Weiss 2012). The purpose of this research was to determine the effects of MMC and rapamycin (RM), a known target of the PI3K-mTOR pathway, as well as to a combination of both agents in the treatment of pancreatic cancer with this genetic background.

To better understand the effects of MMC, RM, and a combination of these treatments, the murine xenograft Avatar model described was applied to a metabolomics study employing both gas chromatography–mass spectrometry (GC-MS) and liquid chromatography–mass spectrometry (LC-MS). The aim of the study was to reveal phenotypic effects of each treatment and to propose why MMC was the most effective treatment, while other treatments were less effective. For both analytical platforms, pancreatic extract samples were prepared from the murine xenografts in four different experimental groups: those treated with MMC, RM, MMC+RM or not treated (NT). Samples were collected in triplicate from three different mice in each group resulting in nine replicates and metabolite extracts from each were analyzed using both mass spectrometry techniques. The approach involved metabolic fingerprinting, a top-down approach to reveal phenotypic information with no particular expectations regarding the metabolomes of each group.

The relative concentrations of many metabolites in the xenograft tumors were found to be increased by MMC relative to the other treatment groups, including a number that are involved in central carbon metabolism (CCM).

Materials and Methods

An avatar mouse model (JH033) from a patient with pancreatic cancer and mutations in the *PALB2* and *TSC2* genes and this system was used for these experiments. Immunocompromised mice (Harlan, Sant Feliu de Codines, Spain) between 4 and 6 weeks of age were housed on irradiated corncob bedding (Teklad, Sant Feliu de Codines, Spain) in individual HEPA-ventilated cages (Sealsafe® Plus, Techniplast, Buguggiate, Italy) on a 12-h light–dark cycle at 21–23°C and 40–60% humidity. Mice were fed water and libitum (reverse osmosis, 2 ppm Cl_2) and an irradiated standard rodent diet (Teklad 2919) consisting of 16% protein, 4% fat, and 4% fiber. Animals were implanted bilaterally on the right and left flank with tumor fragments. Prestudy tumor volumes were recorded for each experiment beginning 1 week prior to its estimated start date. When tumors reached ~150–250 mm³; animals were matched by tumor volume into treatment and control groups and dosing was initiated. Mice were ear tagged and followed individually throughout the experiment. MMC was administered at a dose of 5 mg/kg i.p. from day 1 and RM at a dose of 4 mg/kg daily for 10 days by oral gavage (p.o.). The study protocol was reviewed and approved by the Institutional Animal Care and Use Committee (IACUC). During the study, both the care and use of animals were conducted in accordance with the regulations of the Association for Assessment and Accreditation of Laboratory Animal Care (AAALAC). After inoculation, the animals were checked daily for morbidity and mortality including mobility, food and water consumption, body weight gain/loss (body weights were measured twice weekly or every other day), eye/hair matting, and any other abnormal effect. Death and observed clinical signs were recorded on the basis of the

numbers of animals within each subset. Tumor sizes were measured twice weekly in two dimensions using a calliper, and the volume was expressed in mm^3 using the formula TV = width^2 × length × 0.5. At study completion, tumor growth inhibition (% TGI) values were calculated and reported for each treatment group (T) versus control (C) using initial (i) and final (f) tumor measurements by the equation: % TGI = 1 − [(Tf − Ti)/(Cf − Ci)]. TGI were compared between treated and control groups using a two-tailed "*t*-test.", where $P < 0.05$ was considered statistically significant.

Chemicals

Information regarding all reagents and solvents used in this study are described in Data S1.

Metabolic fingerprinting by GC- and LC-MS

Metabolic fingerprinting of tissue samples (36 samples: 9 per treatment) was performed using both GC- and LC-MS. Full methods are supplied in Data S1 for the preparation of samples, fingerprinting, and data processing by each technique.

Data analysis

Samples were divided into four groups relating to the treatment (MMC, MMC+RM, RM, NT), and compared. Comparison of groups was performed according to the different effect of the treatments under study. Firstly, a comparison was made between MMC-treated tumors versus all other experimental groups collectively. Subsequently, the metabolic fingerprints from tumors treated with MMC were compared to the metabolic profiles from tumors treated with the combined MMC and RM treatment, with RM or to NT samples. All four comparisons were used to elucidate the mode of action of MMC with regard to its effect on tumor metabolism.

Differences between metabolites in different groups were evaluated by univariate data analysis followed by a multivariate analysis. Univariate analyses were performed using unpaired *t*-tests with *P*-value <0.05 to consider metabolites with significant differences in the mean peak area for every metabolite between the groups. For each biological comparison, the *P*-values from both LC-MS and GC-MS analyses were collectively corrected using the Benjamini and Hochberg (1995) approach to control the false discovery rate.

Subsequently for classification, multivariate analysis was performed using SIMCA P+ 12.0.1 software (Umetrics, Umeå, Sweden). Principal components analysis (PCA) and orthogonal partial least squares regression discrimi-

nant analysis (OPLS-DA) were performed on log transformed and Pareto scaled data (LC-MS) or non-transformed, UV-scaled data (GC-MS). Transformation and scaling of data were chosen based on suitability for each dataset. To detect trends, outliers, and the quality of the data acquisition, PCA was performed. To discriminate between groups and to identify the compounds responsible, the supervised methods OPLS-DA were performed. All OPLS-DA models were cross-validated by internal cross-validation (CV1) in SIMCA P+. Finally, the percentage of change, using MMC group as control, was calculated for statistically significantly different metabolites of each comparison.

Results

Effect of the treatment in the morphometry of the tissue

Figure 1 shows the TGI curves of Avatar models treated with the agents at the indicated doses and schedules. As expected, MMC was very effective with a TGI of 104%. However, RM showed only moderate activity with a TGI of 64%. Unexpectedly, the combination was ineffective with a TGI of 31% suggesting that blocking of mTOR induced resistance to the DNA damaging actions of MMC.
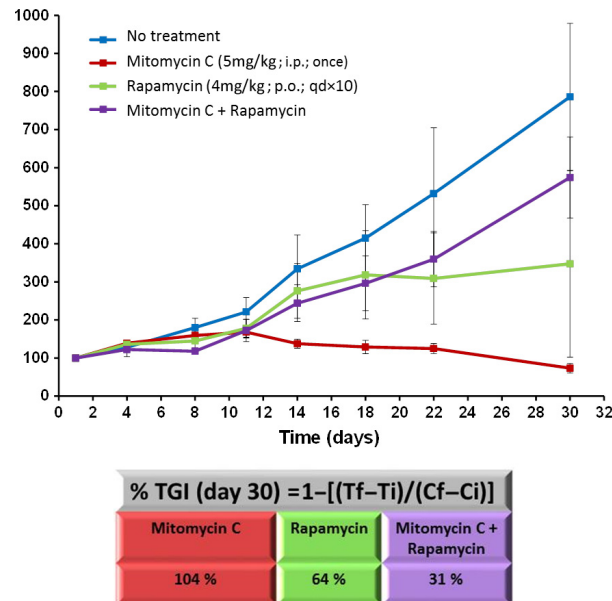
Figure 1. Tumor growth profiles of Avatar model JH033 treated with Mitomycin C and rapamycin. The graph shows the relative tumor volume measured at 8 time points (%, with respect to the tumor volume at the treatment day 1) of the four experimental groups as described in the graph legend. The tumor growth inhibition (TGI), calculated at treatment day 30, is also shown. (MMC, Mitomycin C; i.p., intraperitoneal; p.o., per os; qd×10, every day during 10 days).

Statistical analysis and modeling

LC-MS

The alignment of all masses detected from quality controls (QCs) and pancreas extract samples was the first step of data treatment. This was performed for retention time (RT) in the range 0.48–36 min, where the RT window was 0.5 min and the mass window was 20 ppm. This alignment step generated the data matrix with abundances for 57,936 potential compounds in the first comparison (all other groups [OG] versus MMC), 45,902 for the MMC+RM versus MMC comparison, 48,595 for the RM versus MMC comparison, and 49,877 for the NT versus MMC comparison.

The effect of random signals was minimized using a filter that includes only features present in a minimum number of samples in one of the groups (75%). After filtering, the data matrix contained 1718 different variables for the OG versus MMC comparison, 2035 for MMC+RM versus MMC, 1979 for RM versus MMC, and 2213 for the NT versus MMC comparison.

Univariate analysis (*t*-tests) revealed 318 variables with significant differences in the mean between OG versus MMC, 495 between MMC+RM versus MMC, 517 between RM versus MMC, and 789 between NT versus MMC. These variables were used in multivariate analysis (SIMCA P+ 12.0.1 software). The PCA model was estimated to check the grouping of samples and also to test the quality of the analysis. The PCA plots displayed in Figure 2A show clustering of QC samples in both analyses and neither contained statistical outliers.

To preserve the characteristics of each group and maximize significant difference, a supervised model was required. Four OPLS-DA models were evaluated to explain the differences in the comparisons: OG versus MMC, MMC+RM versus MMC, RM versus MMC, and NT versus MMC. All OPLS-DA models show good separation between groups with strong R^2 and Q^2 coefficients and no outliers can be observed in the Hotelling diagrams (Fig. 2B). To evaluate the significant variables for each OPLS-DA model, a Jackknifed confidence interval estimative with a 95% level of confidence was performed.

A list of 176 variables were obtained and compared in the OG versus MMC after Jackknifed confidence interval test. A total of 266 variables were obtained from the MMC+RM versus MMC comparison, 266 between RM versus MMC, and 277 between NT versus MMC after Jackknifed confidence interval test. All these variables were checked against MASSTRIX and the METLIN database and where possible, putative identifications were assigned.

GC-MS

There was one analytical outlier observed in the GC-MS data and therefore this sample was not processed as the others and was not included in statistical analysis. This sample was in the RM-treated experimental group. GC-MS data, processed by AMDIS and MPP, provided 140 identified and aligned compounds. Among these metabolites, 4 (i.e., from solvent, fatty acid methyl ester (FAME) mix, blanks), 19 (with low abundant and steady peaks), and 9 (AMDIS false-positive identification) were excluded. Then, data were filtered by frequency keeping the compounds present at least in the 75% of the compared groups and nine additional compounds were rejected. Subsequently, missing values were imputed, the 32 derivatives summed, and the data normalized by the IS (methyl stearate). From the 99 compounds obtained in the previous steps, 48 (MMC vs. NT), 31 (OG vs. MMC), 23 (RM vs. MMC), and 27 (MMC+RM vs. MMC) were found to be statistically significant in the *t*-test ($P < 0.05$) and were used in the multivariate data analysis.

As for LC-MS, the four groups under investigation (MMC, MMC+RM, RM, and NT) were compared by OPLS-DA analysis (Fig. 2C). The metabolites responsible for the discrimination after Jackknifed confidence interval were: 48 (MMC vs. NT), 30 (OG vs. MMC), 22 (RM vs. MMC), and 27 (MMC+RM vs. MMC). Tables 1–4 summarize the most significant metabolites identified in both GC-MS and LC-MS from statistical analysis of each comparison described.

Discussion and Conclusions

Biological significance of putative biomarkers

The most effective treatment was observed in pancreatic tumor xenografts treated with MMC. It was shown previously in a patient with advanced pancreatic cancer exhibiting a biallelic inactivation of the DNA repair gene: *PALB2*, that MMC is a highly effective DNA damaging agent for reducing tumor size and prolonging prognosis (Villarroel et al. 2011). This is a key example of the success of personalized cancer treatment and following *PALB2* gene sequencing in other patients, if they too exhibit similar genotypes, it is likely that MMC can also be successful in their treatment. It is possible that as a consequence of increased DNA damage, MMC also causes metabolic effects that could be biomarkers of the pancreatic tumor response. Interestingly, the combination of MMC and RM gave significantly worst results than MMC alone against the expectations. To elucidate the effect of MMC
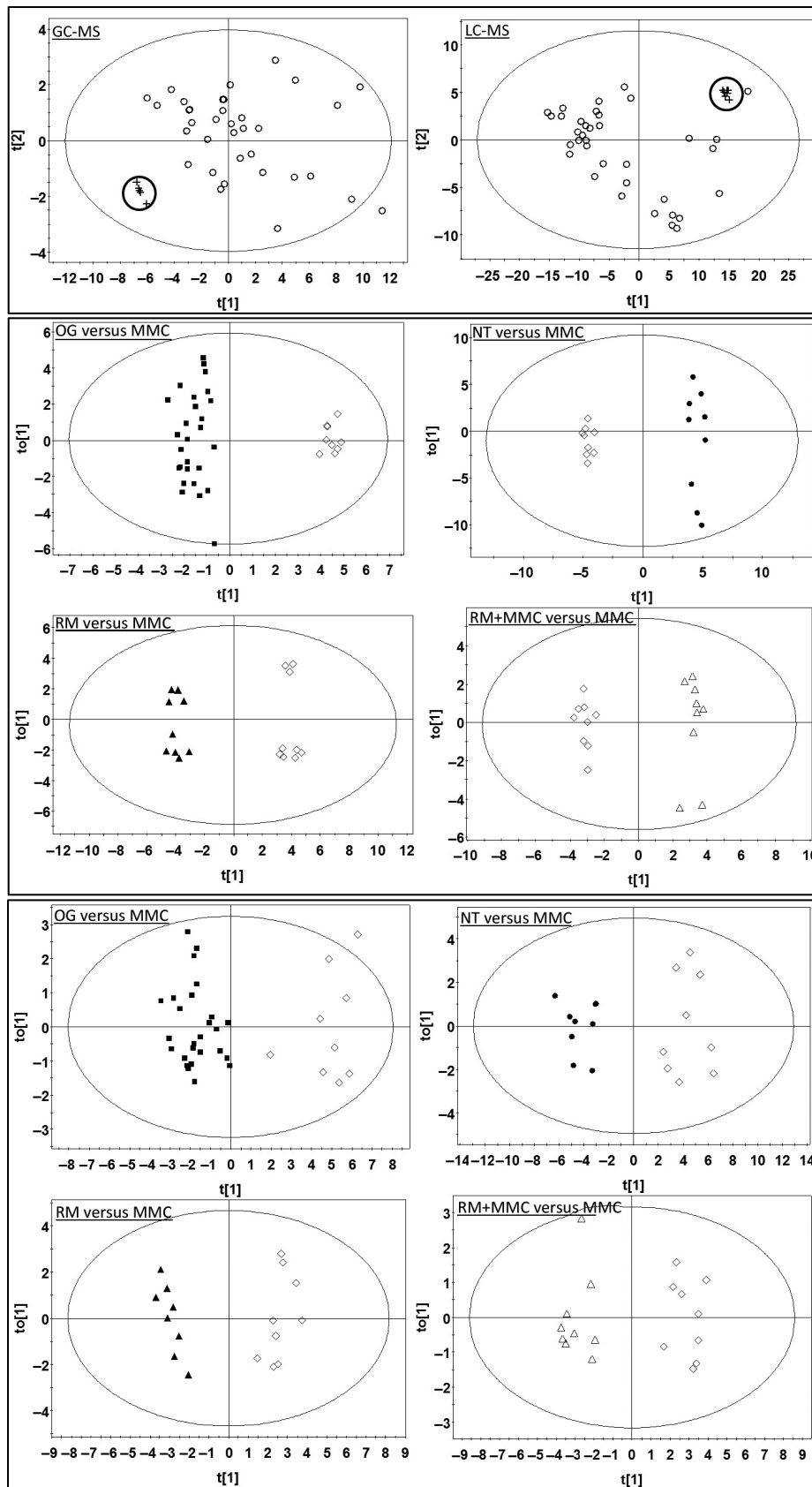
on pancreatic tumor metabolism, these tumors were compared to other treatments to reveal the metabolic differences owed to the effectiveness of MMC. Tables 1–4 highlight the results from these comparisons showing which metabolites are significantly increased or decreased with MMC relative to other treatments.

Firstly, a comparison was made between MMC-treated tumors versus all other experimental groups collectively (Table 1). Subsequently, the metabolic profiles from tumors treated with MMC were compared to the metabolic profiles from tumors treated the combined MMC and RM treatment (Table 2) or with RM (Table 3) as well as to tumors that received no treatment (Table 4). All four comparisons were used to elucidate the mode of action of MMC with regard to its effect on tumor metabolism.

Observing the effects of treatments through metabolomics is highly valuable in personalized medicine as it allows the specific assessment of their action on the phenotype of the patient in question. The treatments presented in this research are not novel themselves; however, their effect on this specific phenotype and their final effects on metabolic phenotype are. The results presented highlight the potential of metabolomics in assessing personalized medicines and reveal the potential of drug repurposing in personalized medicine.

Many of the significant differences between the metabolic profiles of MMC-treated tumors and any other tumors were features of, or features associated with, CCM. This is a vital metabolic subnetwork in cancer metabolism and has been explored extensively over decades of cancer research (Warburg et al. 1927; Richardson et al. 2008). It centers on glycolysis and the tricarboxylic acid (TCA) cycle and involves other pathways that either deliver molecules to be catabolized to produce energy, or that use the carbon for the biosynthesis of other compounds. These connected pathways include the pentose phosphate pathway, amino acid metabolism, purine metabolism, fatty acid biosynthesis, and lipid metabolism including the synthesis of (glyco)sphingolipids and ceramide metabolism. MMC treatment was associated with significant alterations in the concentrations of metabolites from all of these pathways and therefore can be considered to have a relatively broad-spectrum action. This could explain why the treatment is so effective, such that a range of vital processes are targeted. The increase in CCM metabolites that was observed could be indicative that Mytomycin C directly inhibits pathways such as the TCA cycle and that in the absence of efficient cycling, metabolites accumulate. Alternatively, it could be that in response to the treatment, tumors focus their metabolism to conserve vital pathways and suspend functions such as lipid synthesis that may not be crucial for tumor survival.

Carnitine and acylcarnitines were revealed as significant changes in the responses of this metabolic phenotype to MMC. They are important precursors in energy metabolism and are essential for the transport of long-chain fatty acids (Malaguarnera et al. 2006). The concentration of (acyl)carnitines and carnitine precursors such as lysine and methionine can vary depending on intake from diet or alterations in their endogenous biosynthesis (Malaguarnera et al. 2006). In this case, it is likely that MMC alters the synthesis of acylcarnitines and that different derivatives are more or less significant depending on which treatment it is compared to. When compared to RM treatment and OG collectively, MMC appears to increase acylcarnitines. When compared to the combined treatment, MMC increases two acylcarnitines but the combined treatment increases three. Furthermore, the latter are associated with a higher percent change from the combined treatment. It is known that CPT1, an enzyme catalyzing the reaction converting carnitine and acetyl-coA to acylcarnitine, causes a resistance to RM and that it induces fatty acid oxidation (Fingerhut et al. 2001). If MMC is able to upregulate the activity of this enzyme, it could explain why acylcarnitines are increased with MMC relative to RM treatments, but also could provide evidence for why RM seems to be inhibited in the combined treatment since CPT1 involves resistance to RM. Further evidence to support this is that in any comparison highlighting significant difference in fatty acids, they are always decreased with MMC, which could suggest that fatty acid oxidation is elevated with this treatment.

Figure 2. Multivariate analysis of metabolic fingerprints. (A) Principal components analysis (PCA) plots generated from all the samples including the quality controls (QC) samples in gas chromatography–mass spectrometry (GC-MS) and liquid chromatography–mass spectrometry (LC-MS) experiments.○ – All samples + Quality controls. GC-MS model ($R^2 = 0.836$, $Q^2 = 0.708$) for all samples ($n = 35$) and QCs ($n = 5$); LC-MS model ($R^2 = 0.746$, $Q^2 = 0.594$) for all samples ($n = 36$) and QCs ($n = 7$). (B) Orthogonal partial least squares regression discriminant analysis (OPLS-DA) plots generated from the different comparisons under investigation (LC-MS). ■ – Other groups ($n = 27$) ◇ – Mitomycin C (MMC) ($n = 9$) ● – No treatment ($n = 9$) ▲ – Rapamycin (RM) ($n = 9$) ∆ – RM + MMC ($n = 9$). Other groups (OG) versus MMC model ($R^2X = 0.589$, $R^2Y = 0.965$, $Q^2 = 0.778$); not treated (NT) versus MMC model ($R^2X = 0.687$, $R^2Y = 0.991$, $Q^2 = 0.973$); RM versus MMC model ($R^2X = 0.655$, $R^2Y = 0.985$, $Q^2 = 0.931$); RM+MMC versus MMC model ($R^2 = 0.639$, $R^2Y = 0.986$, $Q^2 = 0.933$). (C) OPLS/O2PLS-DA plot generated from the different comparisons under investigation (GC-MS). ■ – Other groups ($n = 27$) ◇ – MMC ($n = 9$) ● – No treatment ($n = 9$) ▲ – RM ($n = 8$) ∆ – RM + MMC ($n = 9$). OG versus MMC model ($R^2X = 0.827$, $R^2Y = 0.898$, $Q^2 = 0.684$); NT versus MMC ($R^2X = 0.791$, $R^2Y = 0.925$, $Q^2 = 0.76$); RM versus MMC model ($R^2X = 0.783$, $R^2Y = 0.96$, $Q^2 = 0.861$); RM+MMC versus MMC model ($R^2X = 0.889$, $R^2Y = 0.947$, $Q^2 = 0.555$).

Table 1. OG versus MMC.

Associated pathway	Metabolite	Technique	Target ion *m/z* (GC) − *MW* (LC)	RT (min)	% Change	*P*-value
Pentose phosphate pathway/ glycolysis	Glycerol-1-phosphate	GC-MS	357	15.93	−47	0.01
	Ribulose-5-phosphate	GC-MS	357	19.52	−40	0.02
	Glucose-6-phosphate	GC-MS	73	21.31	−69	0.004
Purine metabolism	Hypoxanthine	GC-MS	265	16.44	−37	0.01
	Xanthine	GC-MS	353	18.57	−50	0.004
TCA cycle	Succinate	GC-MS	147	10.46	−42	0.002
	Malate	GC-MS	147	12.73	−30	0.04
	(Iso)citrate	GC-MS	273	16.54	−38	0.01
Arginine and proline metabolism/alanine, aspartate and glutamate metabolism	Proline	GC-MS	70	8.62	−26	0.03
	Aspartate	GC-MS	73	11.94	−45	0.009
	Aminomalonate	GC-MS	73	12.51	−48	0.005
	(Pyro)glutamate	GC-MS	156	13.17	−40	0.01
	Glutamine	GC-MS	246	14.30	−40	0.01
	Asparagine	GC-MS	73	14.91	−54	0.005
	Putrescine	GC-MS	174	15.71	−49	0.01
	Ornithine	GC-MS	142	16.55	−59	0.005
Phenylalanine metabolism	Phenylalanine	GC-MS/LC-MS	120/165.0792	13.54/0.75	−38/−24	0.009/0.03
	Phenylpyruvate	LC-MS	164.047	0.69	−24	0.01
	Tyrosine	GC-MS/LC-MS	179/181.0739	17.30/0.7	−42/−27	0.0003/0.05
Valine, leucine, and isoleucine degradation	Valine	GC-MS	72	7.3	−35	0.009
	Leucine	GC-MS	86	8.26	−42	0.02
Cysteine and methionine metabolism/glycine, serine and threonine metabolism	Glycine	GC-MS	102	7.74	−40	0.01
	Serine	GC-MS	116	9.69	−44	0.005
	Methionine	GC-MS	104	11.8	−61	0.009
Lysine degradation/carnitine metabolism	Lysine	GC-MS/LC-MS	174/146.1051	17.64/0.57	−58/−23	0.005/0.02
	Pipecolate	LC-MS	129.0802	0.57	−19	0.04
	Stearoylcarnitine	LC-MS	427.3658	21.23	−33	0.05
Fatty acid biosynthesis/beta-alanine metabolism/lipid metabolism	Acetylspermidine	LC-MS	187.1681	0.58	−37	0.01
	Diacetylspermine	LC-MS	286.2371	0.58	−43	0.01
	Uracil	GC-MS	241	10.77	−42	0.005
	LPS (18:1)	LC-MS	523.2922	22.65	106	0.02
	LPS (18:0)	LC-MS	525.3076	25.63	79	0.01
	LPE (22:6)	LC-MS	525.2853	18.11	72	0.01
	LPE (22:4)	LC-MS	529.3174	21.1	49	0.01
	PC (30:1)/PE (33:1)	LC-MS	703.5113	19.36	55	0.04
	PC (38:6)/PE (41:6)	LC-MS	805.5685	21.57	202	0.05
	PC (34:4)/PE (37:4)	LC-MS	753.5309	34.86	107	0.05
	PG (34:1)	LC-MS	765.5590	31.56	130	0.01

Metabolites found to be statistically significantly different in all other groups compared to Mitomycin C. All *P*-values are those corrected using the Benjamini–Hochberg approach for control of false discoveries. GC-MS, gas chromatography–mass spectrometry; LC-MS, liquid chromatography–mass spectrometry; MMC, Mitomycin C; OG, other groups.

Many amino acids were observed as significant markers of MMC action in this metabolic phenotype. For example, those that function in cysteine and methionine metabolism and/or glycine, serine, and threonine metabolism were also significantly increased in tumors treated with MMC. The metabolic pathway that connects methionine to glycine *via* homocysteine and serine is closely linked with the metabolism of (glycol)sphingolipids and ceramides (Huang et al. 2011). When compared to the combined MMC + RM treatment, MMC increases the concentration of (keto)sphingosine and decreases cera-mide. Similarly, ceramide levels are lower in MMC-treated tumors than in RM-treated tumors. It is known that cellular stress can increase ceramide and that this is a marker of cytotoxicity (Reynolds et al. 2004; Guillermet-Guibert et al. 2009; Huang et al. 2011). The balance between ceramide and sphingosine may shed light on the level or severity of this. Treatments involving RM were associated with an elevation in ceramide, while MMC appeared to increase (keto)sphingosine. This could suggest that RM is more cytotoxic; however, since MMC is known to be more effective, targeting ceramide metabo-

Table 2. MMC+RM versus MMC.

Associated pathway	Metabolite	Technique	Target ion *m/z* (GC) − *MW* (LC)	RT (min)	% Change	*P*-value
Pentose phosphate pathway/	Glycerone phosphate	GC-MS	315	15.73	−58	0.05
glycolysis	Glycerol-1-phosphate	GC-MS	357	15.93	−52	0.007
Purine metabolism	Hypoxanthine	GC-MS	265	16.44	−33	0.03
	Xanthine	GC-MS	353	18.57	−52	0.01
TCA cycle	Succinate	GC-MS	147	10.46	−39	0.009
	Fumarate	GC-MS	245	10.94	−39	0.009
	Malate	GC-MS	147	12.73	−44	0.009
	(Iso)citrate	GC-MS	273	16.54	−37	0.03
Arginine and proline metabolism/	Aspartate	GC-MS	73	11.94	−39	0.04
alanine, aspartate and glutamate	Aminomalonate	GC-MS	73	12.51	−46	0.02
metabolism	(pyro)glutamate	GC-MS	156	13.17	−37	0.02
	Glutamine	GC-MS	246	14.30	−46	0.01
	Asparagine	GC-MS	73	14.91	−57	0.009
	Putrescine	GC-MS	174	15.71	−57	0.004
	Ornithine	GC-MS	142	16.55	−61	0.006
Phenylalanine metabolism	Tyrosine	GC-MS	179	17.3	−31	0.05
Valine, leucine, and isoleucine	Valine	GC-MS	72	7.3	−29	0.03
degradation	Leucine	GC-MS	86	8.26	−36	0.04
Lysine degradation/carnitine	Lysine	GC-MS	174	17.64	−59	0.008
metabolism	Pipecolate	LC-MS	129.0794	0.57	−33	0.002
	Propanoylcarnitine	LC-MS	217.132	0.71	−40	0.002
	Butyrylcarnitine	LC-MS	231.1482	0.75	−25	0.01
	Tetradecanoylcarnitine	LC-MS	371.3029	18.14	−56	0.0006
	Linoelaidyl carnitine	LC-MS	423.3343	17.27	53	0.04
Fatty acid biosynthesis/beta-alanine	Uracil	GC-MS	241	10.77	−44	0.002
metabolism/lipid metabolism	PI (42:0)	LC-MS	936.7118	32.46	59	0.02
	PS (42:0)	LC-MS	875.6528	32.59	65	0.01
	LPE (18:0)	LC-MS	481.3169	23.06	50	0.004
	LPE (22:4)	LC-MS	529.3174	21.11	64	0.01
	LPE (22:5)	LC-MS	527.3037	19.07	57	0.02
	LPE (22:6)	LC-MS	525.2854	18.11	63	0.01
Ceramide and (glyco)sphingolipid	(Keto)sphingosine	LC-MS	285.2695	14.56	−59	0.005
metabolism	NeuAc(α)Gal(β)-Cer(d34:2)	LC-MS	1128.801	27.6	51	0.003
Prostaglandins	Glyceryl-PG D2/E2/H2	LC-MS	426.2588	6.23	−52	0.009
	Methyl-PG A2/D2	LC-MS	348.2276	20.62	82	0.04
	PG A1	LC-MS	318.2171	19.11	−57	0.03

Metabolites found to be statistically significantly different in the combined Mitomycin C and Rapamycin treatment compared to Mitomycin C. All *P*-values are those corrected using the Benjamini–Hochberg approach for control of false discoveries. GC-MS, gas chromatography–mass spectrometry; LC-MS, liquid chromatography–mass spectrometry; MMC, Mitomycin C; RM, rapamycin.

lism is less effective than pathways such as CCM. Sphingosine kinase-1 is a commonly overexpressed enzyme in pancreatic cancer that catalyzes the reaction between ceramide and sphingosine-1-phosphate (Guillermet-Guibert et al. 2009). A phenotype exhibiting elevated sphingosines relative to ceramides due to increased sphingosine kinase activity has been associated with chemoresistance to other chemotherapeutic agents (Guillermet-Guibert et al. 2009). However, although cells may be responding to the treatment in this way (since MMC is effective) it could be that this mechanism for resistance is not successful.

Purine metabolism was highlighted through the significantly higher concentrations of xanthine, hypoxanthine,

and inosine in tumors treated with MMC compared to other treatments. It has been suggested previously that xanthine can serve as an electron donor for the xanthine oxidase catalyzed reduction of MMC; thus, it functions similar to NAD(P)H (Pan et al. 1984).

It was expected that the combination of MMC and RM would be more effective than MMC alone; however, it may be possible that these drugs counteract each other. For example, RM is known to target the PI3K-mTOR pathway. This pathway is involved in a multitude of biological processes related to cell growth and metabolism. In particular, the role of mTOR in lipid biosynthesis has been reviewed (Laplante and Sabatini 2009). Since RM

Table 3. RM versus MMC.

Associated pathway	Metabolite	Technique	Target ion *m/z* (GC) − *MW* (LC)	RT (min)	% Change	*P*-value
Pentose phosphate pathway/glycolysis	Glucose-6-phosphate	GC-MS	73	21.31	−74	0.6*
Purine metabolism	Hypoxanthine	GC-MS	265	16.44	−36	0.03
	Xanthine	GC-MS	353	18.57	−42	0.009
	Inosine	GC-MS	73	23.37	−52	0.1
TCA cycle	Succinate	GC-MS	147	10.46	−44	0.03
Arginine and proline metabolism/alanine, aspartate and glutamate metabolism	Alanine	GC-MS	116	7.47	−46	0.03
	Aspartate	GC-MS	73	11.94	−37	0.001
	Aminomalonate	GC-MS	73	12.51	−43	0.05
	Ornithine	GC-MS	142	16.55	−49	0.03
Phenylalanine metabolism	Phenylalanine	GC-MS	120	13.54	−39	0.2*
	Tyrosine	GC-MS	179	17.3	−39	0.03
Valine, leucine, and isoleucine degradation	Valine	GC-MS	72	7.3	−31	0.03
Cysteine and methionine metabolism/ glycine, serine and threonine metabolism	Glycine	GC-MS	102	7.74	−35	0.04
	Serine	GC-MS	116	9.69	−46	0.2*
	Methionine	GC-MS	104	11.8	−71	0.1*
Lysine degradation/carnitine metabolism	Lysine	GC-MS	174	17.64	−38	0.05
	Pipecolate	LC-MS	129.0794	0.57	−25	0.001
	Methylbutyroyl-carnitine	LC-MS	245.1637	0.78	−38	0.01
Fatty acid biosynthesis/beta-alanine metabolism/lipid metabolism	10-hydroxycaprilate	GC-MS	73	16.33	−71	0.04
	Acetylspermidine	LC-MS	187.1682	0.58	−44	0.003
	Linolenate	LC-MS	278.2245	26.11	67	0.04
	Anandamide (18:3)	LC-MS	321.2669	28.19	64	0.003
	Octadecylphosphocholine	LC-MS	435.3546	32.4	29	0.05
	PC (20:1)	LC-MS	563.3495	0.82	−49	0.003
	PC (36:6)/PE (39:6)	LC-MS	777.5306	31.18	71	0.04
	PG (43:4)	LC-MS	868.6138	0.8	−35	0.005
	LPC (18:2)	LC-MS	519.3309	18.88	173	≈0
	LPC (18:3)	LC-MS	517.315	16.23	68	0.001
	LPC (20:4)	LC-MS	543.3325	18.33	58	0.02
	LPC (20:5)	LC-MS	541.317	15.83	33	0.03
	LPC (22:5)	LC-MS	569.3476	19.24	62	0.02
	LPS (18:1)	LC-MS	523.2927	22.65	103	0.01
	LPS (18:2)	LC-MS	521.276	19.46	92	0.04
Ceramide and (glyco)sphingolipid metabolism	LacCer(d38:0)	LC-MS	919.6808	32.48	68	0.05
	NeuAc(α)Gal(β)-Cer(d44:2)	LC-MS	1128.801	27.6	27	0.05
	Ganglioside GM3 (d18:0/22:0)	LC-MS	1238.813	35.62	76	0.03
Prostaglandins	Glyceryl-PG D2/E2/H2	LC-MS	426.2586	6.25	−43	0.03

Metabolites found to be statistically significantly different in the Rapamycin treatment compared to Mitomycin C. All *P*-values are those corrected using the Benjamini–Hochberg approach for control of false discoveries. *P*-values marked with an asterisk were found to be significant in the *t*-tests but not after false discovery correction. Since they relate to other metabolites in key biological pathways, they are displayed in the table for reference. GC-MS, gas chromatography–mass spectrometry; LC-MS, liquid chromatography–mass spectrometry; MMC, Mitomycin C; RM, rapamycin.

blocks the PI3K-mTOR pathway in a way that should inhibit the biosynthesis of lipids, it would be expected that lipids not be exposed as features in groups involving RM treatment. However, the converse was true. A range of lipids including fatty acids, triglycerides, lysophosphoethanolamines, phosphatidylinositol, phosphatidylerines and phosphocholines were found to be significantly lower in MMC-treated tumors than in RM-treated tumors. This could suggest that RM is less effective than MMC at reducing lipid synthesis or that MMC inhibits the action of RM on the PI3K-mTOR pathway.

Fatty acids such as octadecanoic acid, hexadecanoic acid, nonadecadienoic acid and tetradecanoic acid were significantly reduced with MMC compared to tumors that received no treatment. Fatty acid synthase (FAS), which is used to catalyze the synthesis of many fatty acids and is commonly overexpressed in solid tumors, has been previously described as a marker of pancreatic adenocarcinoma (Walter et al. 2009). This explains why the concentration of fatty acids is elevated in the nontreated pancreatic tumor samples and suggests that MMC may be effective in reducing the activity of FAS in a way to reduce tumor function.

Table 4. NT versus MMC.

Associated pathway	Metabolite	Technique	Target ion *m/z* (GC) − *MW* (LC)	RT (min)	% Change	*P*-value
Pentose phosphate pathway/glycolysis	Pyruvate	GC-MS	174	6.7	−42	0.02
	Lactate	GC-MS	147	6.85	−34	0.03
	Glycerone phosphate	GC-MS	315	15.73	−72	0.008
	Glycerol-1-phosphate	GC-MS	357	15.93	−56	0.004
	Ribulose-5-phosphate	GC-MS	357	19.52	−72	0.004
	Glucose-6-phosphate	GC-MS	73	21.31	−86	0.001
	6-phospho-gluconate	GC-MS	73	22.2	−49	0.04
Taurine and hypotaurine metabolism	Hypotaurine	GC-MS	188	14.13	−72	0.003
Purine metabolism	Hypoxanthine	GC-MS	265	16.44	−41	0.01
	Xanthine	GC-MS	353	18.57	−57	0.003
	Inosine 5′-monophosphate	GC-MS	315	26.86	−56	0.02
TCA cycle	Succinate	GC-MS	147	10.46	−42	0.02
	Fumarate	GC-MS	245	10.94	−46	0.02
	Malate	GC-MS	147	12.73	−49	0.009
	(Iso)citrate	GC-MS	273	16.54	−62	0.007
Arginine and proline metabolism/alanine, aspartate and glutamate metabolism	Aspartate	GC-MS	73	11.94	−59	0.002
	Aminomalonate	GC-MS	73	12.51	−54	0.006
	(pyro)glutamate	GC-MS	156	13.17	−58	0.003
	Creatinine	GC-MS	115	13.58	−31	0.04
	Glutamine	GC-MS	246	14.30	−51	0.006
	Asparagine	GC-MS	73	14.91	−56	0.005
	Putrescine	GC-MS	174	15.71	−60	0.009
	Ornithine	GC-MS	142	16.55	−66	0.004
Butanoate metabolism	3-Hydroxybutanoate	GC-MS	147	8.29	−75	0.0009
Phenylalanine metabolism	Phenylalanine	GC-MS	120	13.54	−48	0.004
	Tyrosine	GC-MS	179	17.31	−56	0.0002
Valine, leucine and isoleucine degradation	Valine	GC-MS	72	7.3	−45	0.004
	Leucine	GC-MS	86	8.26	−57	0.01
Cysteine and methionine metabolism/ glycine, serine and threonine metabolism	Glycine	GC-MS	102	7.74	−55	0.003
	Serine	GC-MS	116	9.69	−60	0.0003
	Methionine	GC-MS	104	11.8	−73	0.004
Lysine degradation/carnitine metabolism	Lysine	GC-MS	174	17.64	−74	0.0004
	ʟ-Octanoylcarnitine	LC-MS	287.2089	4.09	27	0.05
	Palmitoylcarnitine	LC-MS	399.3328	15.87	59	0.002
Fatty acid biosynthesis/beta-alanine metabolism/lipid metabolism	Uracil	GC-MS	241	10.77	−48	0.001
	ᴏ-phosphocolamine	GC-MS	73	16.18	−53	0.01
	Myristate	GC-MS	285	16.91	99	0.01
	Palmitate	GC-MS	117	18.88	114	0.01
	Oleate	GC-MS	339	20.46	108	0.04
	Stearate	GC-MS	117	20.69	85	0.01
	Acetylspermidine	LC-MS	187.1681	0.58	39	0.04
	Nonadecadienoate	LC-MS	294.2557	26.55	578	0.009
	Oxododecenoate	LC-MS	212.1407	14.67	403	0.009
	PS (40:0)	LC-MS	831.622	32.72	43	0.008
	PI (37:0)	LC-MS	866.6626	21.51	40	0.008
	PC (43:6)/PE (46:6)	LC-MS	875.6528	32.58	49	0.007
	PC (13:1)/PE (16:1)	LC-MS	451.2699	18.86	645	0.002
	LPE (16:0)	LC-MS	437.2913	20.26	142	0.008
	LPC (16:1)	LC-MS	493.3166	16.91	130	0.002
	LPE (18:0)	LC-MS	481.3169	23.05	153	0.0005

Metabolites found to be statistically significantly different in the samples that received no treatment compared to Mitomycin C. All *P*-values are those corrected using the Benjamini–Hochberg approach for control of false discoveries. GC-MS, gas chromatography–mass spectrometry; LC-MS, liquid chromatography–mass spectrometry; MMC, Mitomycin C; NT, not treated.
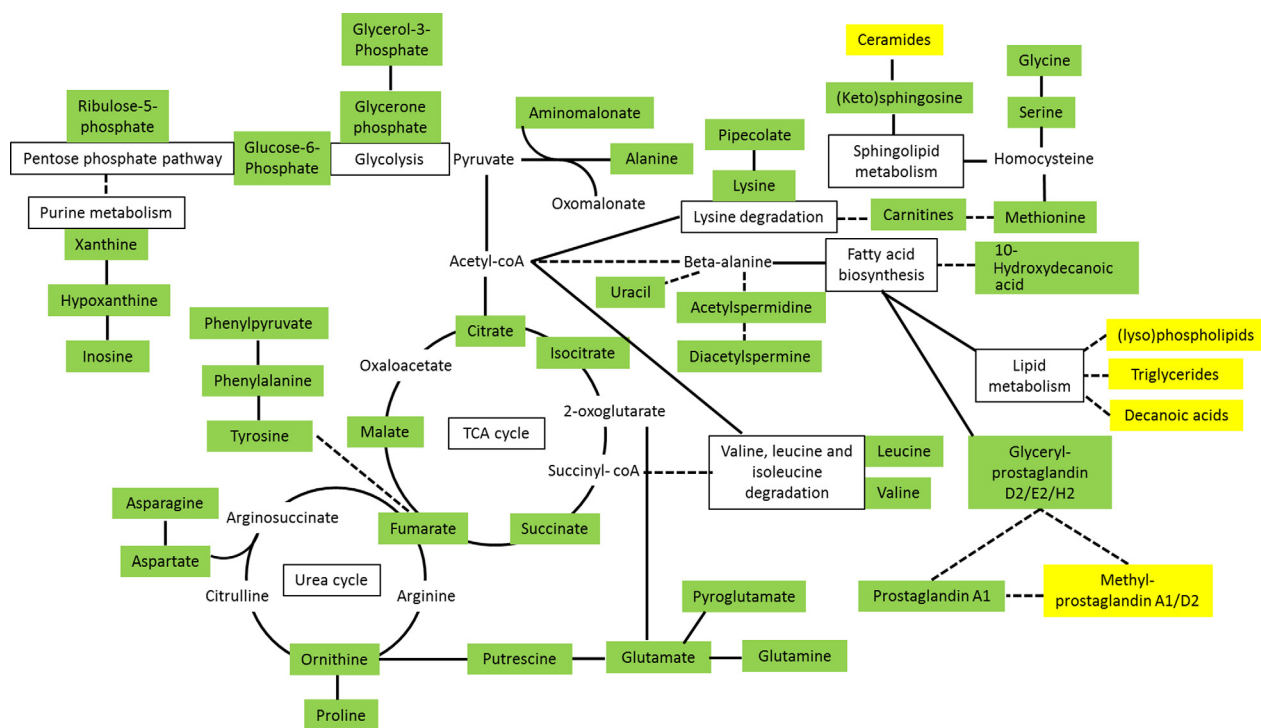
Figure 3. Metabolic network of tumor response to Mitomycin C (MMC) treatment. Colored metabolites were detected using GC/LC-MS and those whose concentrations were increased in response to MMC treatment are highlighted in green and those that decreased in yellow. Several carnitine and (lyso)phospholipids were detected and they are colored to represent the average direction of percentage of change. Metabolites connected by a single reaction are indicated using solid lines and those connected using a dotted line are connected in the same pathway via a range of intermediate metabolites not shown.

The concentration of certain prostaglandins was highlighted as being significantly different between MMC-treated tumors and tumors treated either with RM or the combined MMC + RM treatment. (Glyceryl)prostaglandins were significantly increased by MMC treatment, while methyl-prostaglandins were relatively reduced. The abnormal biosynthesis of prostaglandins from fatty acids has been previously linked with pancreatic cancer development (Ding et al. 2003; Ricciotti and FitzGerald 2011). These are likely to continually increase in the absence of anti-inflammatory agents. There were no significant differences in prostaglandin levels in tumors treated with MMC compared to nontreated tumors, suggesting that MMC has no effect. The increase in prostaglandins in MMC-treated tumors compared to the combined treatment could suggest that the combined treatment involves an anti-inflammatory response that reduces prostaglandin levels in these tumors. Methyl-prostaglandins were present in higher concentrations in tumors treated with the combined therapy relative to MMC alone which could be indicative of the combined therapy utilizing methylation of prostaglandins in its anti-inflammatory response.

MMC treatment increases the concentration of many metabolites in pancreatic tumors. Many of these are involved in CCM and could indicate that MMC directly inhibits CCM or that in response to the treatment, tumors focus their metabolism to conserve vital pathways and suspend extra functions such as lipid biosynthesis. Figure 3 shows the subnetwork of the metabolic effects of MMC treatment in pancreatic tumors. Most of these are increased (highlighted in green) while some are decreased (highlighted in yellow). The interconnecting pathways involved in the subnetwork are marked in boxes and connecting metabolites that were either not detected or not found to be significantly altered by treatment with MMC are shown but are not highlighted. The success of MMC is likely owed to its action in CCM that is relatively broad-spectrum (involving various metabolic pathways).

Acknowledgements

Disclosures

None declared.

References

Benjamini Y, Hochberg Y (1995). Controlling the false discovery rate – a practical and powerful approach to multiple testing. J Roy Stat Soc Ser B Methodol 57: 289–300.

Ding X-Z, Hennig R, Adrian TE (2003). Lipoxygenase and cyclooxygenase metabolism: new insights in treatment and chemoprevention of pancreatic cancer. Mol Cancer 2: 10.

Fingerhut R, Roschinger W, Muntau AC, Dame T, Kreischer J, Arnecke R, et al. (2001). Hepatic carnitine palmitoyltransferase I deficiency: acylcarnitine profiles in blood spots are highly specific. Clin Chem 47: 1763–1768.

Franz DN, Weiss BD (2012). Molecular therapies for tuberous sclerosis and neurofibromatosis. Curr Neurol Neurosci Rep 12: 294–301.

Guillermet-Guibert J, Davenne L, Pchejetski D, Saint-Laurent N, Brizuela L, Guilbeau-Frugier C, et al. (2009). Targeting the sphingolipid metabolism to defeat pancreatic cancer cell resistance to the chemotherapeutic gemcitabine drug. Mol Cancer Ther 8: 809–820.

Hidalgo M (2010). Pancreatic cancer. N Engl J Med 362: 1605–1617.

Huang W-C, Chen C-L, Lin Y-S, Lin C-F (2011). Apoptotic sphingolipid ceramide in cancer therapy. J lipids 2011: 565316.

Jones S, Zhang X, Parsons DW, Lin JC-H, Leary RJ, Angenendt P, et al. (2008). Core signaling pathways in human pancreatic cancers revealed by global genomic analyses. Science 321: 1801–1806.

Laplante M, Sabatini DM (2009). An emerging role of mTOR in lipid biosynthesis. Curr Biol 19: R1046–R1052.

Malaguarnera M, Risino C, Gargante MP, Oreste G, Barone G, Tomasello AV, et al. (2006). Decrease of serum carnitine levels in patients with or without gastrointestinal cancer cachexia. World J Gastroenterol 12: 4541–4545.

Pan SS, Andrews PA, Glover CJ, Bachur NR (1984). Reductive activation of Mitomycin-C and Mitomycin-C metabolites catalyzed by NADPH-cytochrome-P-450 reductase and xanthine-oxidase. J Biol Chem 259: 959–966.

Reynolds CP, Maurer BJ, Kolesnick RN (2004). Ceramide synthesis and metabolism as a target for cancer therapy. Cancer Lett 206: 169–180.

Ricciotti E, FitzGerald GA (2011). Prostaglandins and inflammation. Arterioscler Thromb Vasc Biol 31: 986–1000.

Richardson AD, Yang C, Osterman A, Smith JW (2008). Central carbon metabolism in the progression of mammary carcinoma. Breast Cancer Res Treat 110: 297–307.

Villarroel MC, Rajeshkumar NV, Garrido-Laguna I, De Jesus-Acosta A, Jones S, Maitra A, et al. (2011). Personalizing cancer treatment in the age of global genomic analyses: PALB2 gene mutations and the response to DNA damaging agents in pancreatic cancer. Mol Cancer Ther 10: 3–8.

Vincent A, Herman J, Schulick R, Hruban RH, Goggins M (2011). Pancreatic cancer. Lancet 378: 607–620.

Walter K, Hong S-M, Nyhan S, Canto M, Fedarko N, Klein A, et al. (2009). Serum fatty acid synthase as a marker of pancreatic neoplasia. Cancer Epidemiol Biomark Prev 18: 2380–2385.

Warburg O, Wind F, Negelein E (1927). The metabolism of tumors in the body. J Gen Physiol 8: 519–530.

Supporting Information

Additional Supporting Information may be found in the online version of this article:

Data S1. Material and Methods.